

Low pH and carbonate saturation state in the North Yellow Sea

W.-D. Zhai et al.

Subsurface low pH and carbonate saturation state of aragonite on China side of the North Yellow Sea: combined effects of global atmospheric CO₂ increase, regional environmental changes, and local biogeochemical processes

W.-D. Zhai^{1,2}, N. Zheng¹, C. Huo¹, Y. Xu², H.-D. Zhao^{1,2}, Y.-W. Li¹, K.-P. Zang¹, J.-Y. Wang¹, and X.-M. Xu¹

¹Key Laboratory for Ecological Environment in Coastal Areas (State Oceanic Administration), National Marine Environmental Monitoring Center, Dalian 116023, China

²State Key Laboratory of Marine Environmental Science, Xiamen University, Xiamen 361005, China

Title Page

Abstract

Introduction

Conclusions

References

Tables

Figures

⏪

⏩

◀

▶

Back

Close

Full Screen / Esc

Printer-friendly Version

Interactive Discussion

Received: 31 December 2012 – Accepted: 8 February 2013 – Published: 19 February 2013

Correspondence to: W.-D. Zhai (wdzhai@126.com)

Published by Copernicus Publications on behalf of the European Geosciences Union.

BGD

10, 3079–3120, 2013

Low pH and carbonate saturation state in the North Yellow Sea

W.-D. Zhai et al.

Title Page

Abstract

Introduction

Conclusions

References

Tables

Figures



Back

Close

Full Screen / Esc

Printer-friendly Version

Interactive Discussion



Abstract

Based upon seven field surveys conducted between May 2011 and January 2012, we investigated pH, carbonate saturation state of aragonite (Ω_{arag}), and ancillary parameters on the Chinese side of the North Yellow Sea, a western North Pacific continental margin of major economic importance. Subsurface waters were nearly in equilibrium with air in May and June. From July to October, the fugacity of CO_2 ($f\text{CO}_2$) of bottom water gradually increased to $697 \pm 103 \mu\text{atm}$ and pH decreased to 7.83 ± 0.07 due to respiration/remineralization processes of primary production induced biogenic particles. In November and January, bottom water $f\text{CO}_2$ decreased and pH gradually returned to an air-equilibrated level due to cooling enhanced vertical mixing. The corresponding bottom water Ω_{arag} was 1.74 ± 0.17 (May), 1.77 ± 0.26 (June), 1.70 ± 0.26 (July), 1.72 ± 0.33 (August), 1.32 ± 0.31 (October), 1.50 ± 0.28 (November), and 1.41 ± 0.12 (January). Critically low Ω_{arag} values of 1.0 to 1.2 were mainly observed in subsurface waters in a salinity range of 31.5–32.5 psu in October and November, accounting for $\sim 10\%$ of the North Yellow Sea area. Water mass derived from the adjacent Bohai Sea had a typical water salinity of 30.5–31.5 psu, and bottom water Ω_{arag} values ranged mostly between 1.6 and 2.4. This study showed that the carbonate system in the North Yellow Sea was substantially influenced by global atmospheric CO_2 increase. The community respiration/remineralization rates in typical North Yellow Sea bottom water mass were estimated at $0.55\text{--}1.0 \mu\text{mol O}_2 \text{ kg}^{-1} \text{ d}^{-1}$ in warm seasons, leading to seasonal drops in subsurface pH and Ω_{arag} . Outflow of the Bohai Sea water mass counteracted the subsurface Ω_{arag} reduction in the North Yellow Sea.

1 Introduction

Over the past 200 yr, atmospheric CO_2 concentration has increased from a pre-industrial value of 280 ppmv (parts per million by volume) to a present day value of

BGD

10, 3079–3120, 2013

Low pH and carbonate saturation state in the North Yellow Sea

W.-D. Zhai et al.

Title Page

Abstract

Introduction

Conclusions

References

Tables

Figures

⏪

⏩

◀

▶

Back

Close

Full Screen / Esc

Printer-friendly Version

Interactive Discussion

Low pH and carbonate saturation state in the North Yellow Sea

W.-D. Zhai et al.

Title Page

Abstract

Introduction

Conclusions

References

Tables

Figures

⏪

⏩

◀

▶

Back

Close

Full Screen / Esc

Printer-friendly Version

Interactive Discussion



390 ppmv (WMO/GAW, 2012). Due to sea surface equilibrium with atmosphere, carbonic acid levels in the upper ocean have risen and pH has decreased by approximately 0.1 units since pre-industry (Zeebe et al., 2008; Doney et al., 2009). These processes may threaten many marine species and even whole ecosystems. This is partially because, at a given pressure, temperature, salinity, and alkalinity, pH determines the carbonate saturation state of aragonite (Ω_{arag}) in seawater (based on the calculation program developed by Lewis and Wallace, 1998). Here Ω is defined as the product of the concentrations of calcium and carbonate ions divided by the apparent solubility product (K_{sp}^*) of calcium carbonate, i.e. $\Omega = [\text{Ca}^{2+}][\text{CO}_3^{2-}]/K_{\text{sp}}^*$. When carbonate levels in seawaters drop below saturation ($\Omega_{\text{arag}} < 1$), carbonate biominerals in calcic shells and skeletons may undergo dissolution (Feely et al., 2002, 2010; Gruber et al., 2012).

Previous laboratory and mesocosm studies show that a pH decrease of 0.2 to 0.3 units inhibits or slows calcification in marine organisms, including corals, foraminifera, and some calcareous plankton (Gao et al., 1993; Zeebe et al., 2008). A pH level of 7.8 or lower (on the NIST-traceable scale) has been shown to influence the survival of *Chlamys farreri* (Yuan et al., 2000), which is an extensively cultured scallop species in the Bohai Sea and the North Yellow Sea (NYS). Further, gastropod shells significantly dissolve at pH values of less than 7.6 (on the NIST-traceable scale) in marine ecosystems affected by volcanic CO_2 vents (Hall-Spencer et al., 2008). Negative effects of increasing CO_2 and acidification have been reported widely for many aquatic organisms, including non-calcifying species (Munday et al., 2009, 2010; Baumann et al., 2012; Domenici et al., 2012).

In eutrophicated coastal regions, algae and other biogenetic particles sink to the bottom waters, where they are remineralized through oxygen-consuming processes. The integrated stoichiometry associated with these processes can be roughly characterized by the traditional Redfield equation:



Low pH and carbonate saturation state in the North Yellow SeaW.-D. Zhai et al.

[Title Page](#)[Abstract](#)[Introduction](#)[Conclusions](#)[References](#)[Tables](#)[Figures](#)[⏪](#)[⏩](#)[◀](#)[▶](#)[Back](#)[Close](#)[Full Screen / Esc](#)[Printer-friendly Version](#)[Interactive Discussion](#)

Oxygen-consuming remineralization is associated with a significant release of CO₂, which increases carbonic acid levels in subsurface waters. If local hydrological dynamics cannot enable degassing of the subsurface CO₂, a pH decrease of 0.2 to 0.3 units can occur on seasonal or even intra-seasonal timescales (Cai et al., 2011; Zhai et al., 2012). So far only a few mechanism-involved studies have been designed to understand the integrated effects of global atmospheric CO₂ increase and local respiration/remineralization processes (e.g. Feely et al., 2010; Cai et al., 2011; Sunda and Cai, 2012). In this research, we investigated seasonal variations of pH and Ω_{arag} in the western and central parts of the NYS, revealing controls of subsurface pH/Ω_{arag} dynamics in this continental margin, which will assist future predictions of marine environment changes in the context of ocean acidification. This high quality dataset of Ω_{arag} is the first reported for this important marine aquaculture region.

2 Materials and methods

2.1 Study area

The NYS is a shallow semi-enclosed marginal sea of the western North Pacific, with an area of 71 300 km² and a mean depth of 38 m. It is connected to the Bohai Sea through a narrow channel, while it is relatively open to the South Yellow Sea (Fig. 1). The Bohai Sea has a volume of $1.4 \times 10^{12} \text{ m}^3$ (with an area of 77 000 km² and a mean depth of 18 m), fed by runoff of approximately $89 \times 10^9 \text{ m}^3 \text{ yr}^{-1}$ (Feng et al., 2007), including major runoff contributions from the Yellow River, the largest river in North China. This implies that significant Bohai Sea water mass outflow occurs in flood seasons along the southern shoreline (Fig. 1). Yellow River water has a very high alkalinity of $\sim 3600 \mu\text{mol kg}^{-1}$ before it empties into the Bohai Sea (Wang et al., 2005). This is because of intensive carbonate weathering and evaporation in the Yellow River drainage basin (Chen et al., 2005). Therefore, dynamics of water discharge and alkalinity export

from the Yellow River have significant impacts on the Bohai Sea water mass outflow and thereby on the carbonate system in the adjacent NYS.

The NYS is also surrounded by the Liaoning and Shandong provinces of China, and the Democratic People's Republic of Korea. Liaoning and Shandong provinces are both fast-developing marine aquaculture zones, and highly populated regions of China. Although acidification-sensitive bivalve mollusks of the family *Pectinidae* and echinoderms of the class *Holothuroidea* are of major ecological and economic importance in these NYS coastal ecosystems, thus far information regarding pH and carbonate saturation state in the NYS remains limited.

2.2 Survey design

From May 2011 to January 2012, we conducted seven field surveys (Table 1) in central and western parts of the NYS (Fig. 1). Recently, water flux from the lower Yellow River has been mainly modulated by the manipulation of water discharge from several major dams located 800–1000 km upstream of its estuary (Wang et al., 2011). From January to mid-June in 2011, water discharge remained less than $300 \text{ m}^3 \text{ s}^{-1}$ in the lower Yellow River (Fig. 2). In late June, however, it reached a peak of $\sim 3000 \text{ m}^3 \text{ s}^{-1}$. From mid-July to early September, the water discharge ranged between 190 and $650 \text{ m}^3 \text{ s}^{-1}$, and reached the second peak of $\sim 3000 \text{ m}^3 \text{ s}^{-1}$ in late September. From October 2011 to early January 2012, the mean water discharge was $1070 \pm 300 \text{ m}^3 \text{ s}^{-1}$. Therefore, our surveys were conducted from late spring (May), early summer (June) before human-controlled flooding, mid-summer (July) shortly after the human-controlled flood, and dry late summer (August), to flooding autumn (October and November) and winter (January) (Fig. 2a). During these surveys, water samples for pH, total alkalinity (TALK), dissolved oxygen (DO), and chlorophyll *a* (chl *a*) determination were collected at 8–26 grid stations. Most sampling stations had a water depth of 25–78 m (Fig. 1). The northern sampling stations were near a highly developed marine aquaculture zone around Dalian City (Fig. 1).

BGD

10, 3079–3120, 2013

Low pH and carbonate saturation state in the North Yellow Sea

W.-D. Zhai et al.

Title Page

Abstract

Introduction

Conclusions

References

Tables

Figures

⏪

⏩

◀

▶

Back

Close

Full Screen / Esc

Printer-friendly Version

Interactive Discussion

2.3 Sampling and analyses

Depth profiles of temperature and salinity (Practical Salinity Scale of 1978) were determined with calibrated Conductivity-Temperature-Depth/Pressure (CTD) recorders (SBE911+ in June and in November, and SBE19+ during other surveys, Sea-Bird Co., USA), on board the R/V *Dongfanghong II* (June and November) and the R/V *Yixing* (other survey times). Water samples were obtained at 3–4 depths using rosette samplers fitted with 8 L or 2.5 L Niskin bottles, which were mounted with CTD units. The bottom water samples were collected from a depth of 2 to 5 m above the sea bed.

Water samples for DO analyses were collected, fixed, and titrated on board following the classic Winkler procedure. A small quantity of NaN_3 was added during subsample fixation to remove possible interference from nitrites (Wong, 2012). Based on repeat determinations of the concentration of the $\text{Na}_2\text{S}_2\text{O}_3$ titration reagent used, the uncertainty of the DO data was estimated to be at a satisfactory level of $< 0.5\%$ (Zhai et al., 2012). The DO saturation was calculated from field-measured DO concentration divided by DO concentration at equilibrium with the atmosphere, as per the Benson and Krause (1984) equation and local air pressure.

Water samples for pH analyses were collected on board using a procedure similar to that used for DO. They were preserved with HgCl_2 and determined at 25.0°C within 6 h of sampling. The precision pH analyzer (Orion Star[™], Thermo Electron Co., USA) used was equipped with an Orion[®] 8102BN Ross combination electrode (Thermo Electron Co., USA) against two or three standard buffers. During field surveys, we used two pH buffer sets. The first set included three NIST-traceable buffers, which were used during all surveys. The second set of pH buffers was used only during the June and November surveys, and included two carefully prepared solutions of 2-amino-2-hydroxy-1,3-propanediol (tris) and 2-aminopyridine. These are used by chemical oceanographers as total-hydrogen-ion-scale pH buffers ($\text{pH}_T = -\log_{10}[\text{H}^+]_T$, where $[\text{H}^+]_T = [\text{H}^+] + [\text{HSO}_4^-]$) (Dickson et al., 2007). Based on parallel measurements in June and November using the two pH buffer sets, we concluded that the pH data on the

BGD

10, 3079–3120, 2013

Low pH and carbonate saturation state in the North Yellow Sea

W.-D. Zhai et al.

Title Page

Abstract

Introduction

Conclusions

References

Tables

Figures

⏪

⏩

◀

▶

Back

Close

Full Screen / Esc

Printer-friendly Version

Interactive Discussion

with field measured dissolved inorganic carbon (DIC) and Ca^{2+} data in June, August, and November (Zhai et al., unpublished data), most relative deviations of calculated $\text{DIC}/\text{Ca}^{2+}$ values were at satisfactory levels of $< 1\%$ for DIC (Fig. A2) and $< 2\%$ for Ca^{2+} (plots not reported). These comparison results suggested that our calculated results of carbonate system parameters were reliable.

3 Results

3.1 Environmental settings

Our surveys covered fully four seasons. In January, a typical winter month, water temperature ranged mostly between 3.19°C and 6.74°C (Fig. 3a), although extremely low temperatures between -1.45°C and 0.64°C were also measured at two northern stations. From early spring through to late summer, sea surface temperature (SST) increased from $6.21\text{--}13.22^\circ\text{C}$ in May to $19.22\text{--}24.83^\circ\text{C}$ in July/August (Fig. 3a–d), while the mean bottom water temperature of deep stations (water depth $> 25\text{ m}$, the same below) increased from $5.5 \pm 1.3^\circ\text{C}$ in May to $13.3 \pm 5.0^\circ\text{C}$ in August (Table 1). Therefore, a clear stratification was observed at most stations in those summer months (from June to August) (Fig. 3b–d). Stratification was also observed in October (Fig. 3e), despite the fact that surface waters had cooled to $14.73\text{--}18.37^\circ\text{C}$. In November, SST declined to $11.47\text{--}14.53^\circ\text{C}$ and the temperature induced water stratification was not observed at those northern stations in the area under survey (Fig. 3f).

Compared with the significant seasonal variation of bottom water temperatures at deep stations, bottom water salinity showed only small changes on average (Table 1). However, spatial distributions of bottom water salinity showed seasonal variations (Fig. 4). In May and June, bottom water salinity was $31.5\text{--}32.5\text{ psu}$ at most stations (Fig. 4a, b), which was typical for NYS subsurface waters (Fig. 4). After the human-controlled discharge period in the lower Yellow River in late June (Fig. 2a), however, a tongue-like bottom water mass with relatively low salinity of $30.5\text{--}31.5\text{ psu}$

BGD

10, 3079–3120, 2013

Low pH and carbonate saturation state in the North Yellow Sea

W.-D. Zhai et al.

Title Page

Abstract

Introduction

Conclusions

References

Tables

Figures

⏪

⏩

◀

▶

Back

Close

Full Screen / Esc

Printer-friendly Version

Interactive Discussion

was observed from July to November in the southwestern part of the NYS under survey (Fig. 4c–f). Since salinity of 30.5–31.5 psu is typical for the Bohai Sea in 2011 (Zhai et al., 2012), our southwestern stations may reflect influences of the Bohai Sea water mass on the NYS.

Figure 5 shows the surface chl *a* distributions in May, July, October, and January. On average, surface chl *a* values were measured at $1.96 \pm 1.42 \mu\text{gL}^{-1}$ in May, $1.87 \pm 1.58 \mu\text{gL}^{-1}$ in July, $3.29 \pm 2.70 \mu\text{gL}^{-1}$ in October, and $1.06 \pm 1.01 \mu\text{gL}^{-1}$ in January. Most of these values were higher than the typical surface chl *a* concentration of 0.1–1.0 μgL^{-1} in the oligotrophic northern South China Sea (e.g. Huang et al., 2008). Significantly high values of surface chl *a* were measured at 4 to 7 μgL^{-1} in July in the northern and southwestern parts of the NYS under study, and 11 μgL^{-1} was observed in October in the northern part of the NYS (Fig. 5c), indicating high primary production in the northern and southwestern areas under study. According to the marine environmental status bulletin released by the State Oceanic Administration of China, 7 cases of red tide were recorded in 2011 in the northern part of the NYS (<http://www.mem.gov.cn/gjgb/index.htm>).

Relatively high DO saturation of 110 % to 150 % in surface waters in June and August (Fig. 6a, b) also indicated high primary production in the upper water columns of the NYS. Below the thermocline depths, DO saturation ranged from 87 % to 103 % in June and from 68 % to 95 % in August (Fig. 6a, b). In November, although surface cooling enhanced vertical mixing at several stations and therefore increased bottom water DO to relatively high saturation levels of 85 % to 94 % at several well-mixed northeastern stations, quite low DO saturation values of 50 % to 70 % were detected in bottom waters of most other stations (Fig. 6c), even at several northern temperature-homogeneous stations. In January, DO saturation was measured at 95 % to 105 % (Fig. 6d). Significantly, averaged bottom water DO in deep stations declined from $291 \pm 12 \mu\text{molO}_2 \text{kg}^{-1}$ in June to $227 \pm 24 \mu\text{molO}_2 \text{kg}^{-1}$ in August to $208 \pm 33 \mu\text{molO}_2 \text{kg}^{-1}$ in November (Table 1).

Low pH and carbonate saturation state in the North Yellow Sea

W.-D. Zhai et al.

Title Page

Abstract

Introduction

Conclusions

References

Tables

Figures

⏪

⏩

◀

▶

Back

Close

Full Screen / Esc

Printer-friendly Version

Interactive Discussion



3.2 pH and TAlk

From winter to spring, sea surface pH_T (25°C) varied between 7.67 and 7.92 in January and between 7.85 and 8.11 in May (Fig. 7a). In June and July, sea surface pH_T (25°C) varied between 7.87 and 8.06 (Fig. 7b, c). From late summer to autumn, sea surface pH_T (25°C) varied from 7.88–8.14 in August to 7.86–8.11 in October to 7.76–7.94 in November (Fig. 7d–f). However, subsurface pH_T (25°C) was measured mostly between 7.65 and 7.90 at those stratified stations (Fig. 7). Even during autumn surveys (October and November), very low pH_T (25°C) values of 7.53 to 7.60 were observed in several bottom waters (Fig. 7e, f). Typically, subsurface pH_T (25°C) was lower than surface pH_T (25°C) by 0.2 to 0.4 units at those stratified stations (Fig. 7). At many sampling sites, typically low pH_T (25°C) values of bottom waters were observed at a depth of 20 to 30 m above the sea bed (Fig. 7).

Figure 8 shows the bottom water pH_T (25°C) distributions during surveys in the central and western parts of the NYS. Significantly, very low pH_T (25°C) of 7.53–7.60 dominated in October, reaching a maximum area of $\sim 6150\text{ km}^2$ (Fig. 8e), nearly 10% of the total area of the NYS. In November, bottom water low pH_T (25°C) of < 7.6 only existed at two northern stations (Fig. 8f). A tongue-like bottom water mass with relatively high pH_T (25°C) of > 7.8 was observed in May/June and October/November in the southwestern area under survey (Fig. 8).

Bottom water TAlk was typically measured at $2220\text{--}2310\ \mu\text{mol kg}^{-1}$ (Table 1). To filter the effect of salinity, we proportionally normalized bottom water TAlk to a uniform salinity of 35 psu (NTalk hereafter). Figure 9 shows the typical NTalk value in the western area of the NYS under survey was $2460\text{--}2550\ \mu\text{mol kg}^{-1}$, much higher than the open ocean value of $2300\text{--}2310\ \mu\text{mol kg}^{-1}$ in the nearby western North Pacific (Lee et al., 2006). This was induced by long-term mixing with Bohai Sea waters, which are directly influenced by high-Talk Yellow River input. During most surveys, a tongue-like bottom water mass with a very high NTalk of $2550\text{--}2605\ \mu\text{mol kg}^{-1}$ was usually observed in the southwestern part of the NYS (Fig. 9a–f). This further suggested that the

BGD

10, 3079–3120, 2013

Low pH and carbonate saturation state in the North Yellow Sea

W.-D. Zhai et al.

Title Page

Abstract

Introduction

Conclusions

References

Tables

Figures

⏪

⏩

◀

▶

Back

Close

Full Screen / Esc

Printer-friendly Version

Interactive Discussion

southwestern stations reflected more characteristics of the Bohai Sea waters than did the other stations.

3.3 Carbonate saturation state and bottom water $f\text{CO}_2$

In May and June, typical bottom water Ω_{arag} was calculated at 1.4–2.0 in the central and western parts of the NYS under study (Fig. 10a, b). In July and August, very low Ω_{arag} values of 1.25–1.35 were observed in bottom waters at several western stations (Fig. 10c, d). Similar to the above-mentioned bottom water pH_T distributions (Fig. 8), critically low bottom water Ω_{arag} values of 1.0–1.2 were detected at nine stations (with water depths of 45–70 m) in October (Fig. 10e), accounting for $\sim 10\%$ of the NYS area. In November, critically low bottom water Ω_{arag} values of less than 1.2 were only observed at two northern stations, although very low Ω_{arag} values of less than 1.4 were still dominant in the central and western parts of the NYS (Fig. 10f). In January, the bottom water Ω_{arag} was 1.30–1.88 (Fig. 10g).

Vertical profiles suggested that low Ω_{arag} values of less than 1.8 were generally confined to subsurface waters (below 20 m depth) (Fig. 11). However, they were mixed with surface waters in cooling/cold months (Fig. 11a–f). At many stratified stations, the typical low Ω_{arag} values of bottom waters were also observed at a depth of 20–30 m above the sea bed (Fig. 11). In the above-mentioned tongue-like Bohai Sea water mass, relatively high Ω_{arag} values of 1.8–2.4 were frequently observed (Fig. 10).

Figure 12a shows the seasonal variation of calculated bottom water $f\text{CO}_2$ at the deep stations in the NYS. On average, bottom water $f\text{CO}_2$ increased from nearly air-equilibrated $371 \pm 42 \mu\text{atm}$ in May and $392 \pm 35 \mu\text{atm}$ in June to CO_2 -supersaturated $459 \pm 41 \mu\text{atm}$ in July and $536 \pm 61 \mu\text{atm}$ in August, reaching a peak value of $697 \pm 103 \mu\text{atm}$ in October. In November and January, bottom water $f\text{CO}_2$ declined to $576 \pm 116 \mu\text{atm}$ and $468 \pm 61 \mu\text{atm}$, respectively. When bottom waters were warmed to 25°C , the $f\text{CO}_2$ values increased by 330 to $530 \mu\text{atm}$ (Fig. 12a).

BGD

10, 3079–3120, 2013

Low pH and carbonate saturation state in the North Yellow Sea

W.-D. Zhai et al.

Title Page

Abstract

Introduction

Conclusions

References

Tables

Figures

⏪

⏩

◀

▶

Back

Close

Full Screen / Esc

Printer-friendly Version

Interactive Discussion

4 Discussion

4.1 Major effects of temperature on pH

We calculated pH_T from 25 °C to in situ, based on datasets of TAlk, seawater temperature, and salinity, using the calculation program CO2SYS.xls (Pelletier et al., 2011).

A typical seasonal variation of bottom water pH_T (in situ) at the deep NYS stations was revealed (Fig. 12b), which overall mirrored the seasonal variation pattern of bottom water $f\text{CO}_2$ (Fig. 12a). In May and June, bottom water pH_T (in situ) was 8.08 ± 0.05 and 8.06 ± 0.04 , respectively, close to the present air-equilibrated level of 8.06–8.07. In July and August, it declined to 8.00 ± 0.04 and 7.94 ± 0.04 , respectively. In October, the bottom water pH_T (in situ) reached the lowest value of 7.83 ± 0.07 on average. In November and January, bottom water pH_T (in situ) increased to 7.91 ± 0.08 and 7.98 ± 0.06 , respectively.

According to Gieskes (1969), a temperature increase of 1 °C led to a seawater pH drop of 0.0114 units, since increasing temperature added a greater proportion of free CO_2 than that of CO_3^{2-} in water at a given salinity, TAlk, and pressure. In the NYS, the apparent temperature coefficient of bottom water pH_T in 2011 was estimated at $-0.0144 \text{ pH units } ^\circ\text{C}^{-1}$ ($n = 7$, $r = 0.996$), based on the survey averaged dataset summarized in Table 1. Its absolute value was only a quarter higher than the typical temperature coefficient of seawater pH as suggested by Gieskes (1969). This implied that salinity and TAlk together had minor effects on the pH in the NYS. Based on the dataset of bottom water temperature variation (Table 1), using the two temperature coefficients (-0.0114 and $-0.0144 \text{ pH units } ^\circ\text{C}^{-1}$), we estimated that the effect of temperature on bottom water pH_T accounted for a variation of 0.09–0.11 units in the overall seasonal variation of 0.25 units in 2011.

In contrast, temperature only had minor effects on bottom water Ω_{arag} in the NYS (Fig. 12c). If we calculated bottom water Ω_{arag} from in situ to 5 °C and 15 °C, based on the datasets of TAlk, pH_T (in situ), seawater temperature, and salinity, relative changes in Ω_{arag} ranged between –3% and 5%. The effect of temperature on bottom water

BGD

10, 3079–3120, 2013

Low pH and carbonate saturation state in the North Yellow Sea

W.-D. Zhai et al.

Title Page

Abstract

Introduction

Conclusions

References

Tables

Figures

⏪

⏩

◀

▶

Back

Close

Full Screen / Esc

Printer-friendly Version

Interactive Discussion



Ω_{arag} only accounted for a variation of less than 0.09 on the overall seasonal variation of 0.45 in 2011 (Fig. 12c).

4.2 Responses of pH and Ω_{arag} to $f\text{CO}_2$ increases

Based on TALK, seawater temperature, and salinity datasets (Table 1), and using the calculation program CO2SYS.xls (Pelletier et al., 2011), we calculated seasonal variations of bottom water pH_T and Ω_{arag} under three constant $f\text{CO}_2$ levels of 270 μatm , 380 μatm , and 700 μatm , representing the different air-equilibrated states of pre-industry, present day, and a future scenario by the end of this century. Under different $f\text{CO}_2$ levels, pH_T (in situ) in the NYS was calculated at 8.19–8.20 ($f\text{CO}_2 = 270 \mu\text{atm}$), 8.06–8.07 ($f\text{CO}_2 = 380 \mu\text{atm}$), and 7.82–7.83 ($f\text{CO}_2 = 700 \mu\text{atm}$), respectively (Fig. 12b). Therefore, air-equilibrated pH levels in the NYS declined by 0.13 pH units since the pre-industrial period, similar to the global mean rate of sea surface pH reduction due to the continuous increase of atmospheric CO_2 (Zeebe et al., 2008; Doney et al., 2009). By the end of this century, the air-equilibrated pH may decrease by more 0.24 pH units (Fig. 12b), meaning an increase in total-hydrogen-ion concentrations of 130 % as compared with the pre-industrial period.

Similar to pH, air-equilibrated Ω_{arag} in the NYS declined significantly by 0.6 from pre-industrial to present day (Fig. 12c). By the end of this century, the air-equilibrated Ω_{arag} may reach a critically low level of 1.00–1.37 in the NYS (Fig. 12c).

Figure 12 suggests that the seasonal variation of bottom water pH_T (in situ) was mainly driven by $f\text{CO}_2$. The seasonal variation of bottom water Ω_{arag} was different (Fig. 12c). Although differences between air-equilibrated Ω_{arag} and survey averaged bottom water Ω_{arag} (in situ) were positively correlated with the survey mean bottom water $f\text{CO}_2$ (in situ) (plots not reported), seasonal variation of bottom water Ω_{arag} was only partially dominated by $f\text{CO}_2$. As discussed above, temperature had major effects on $f\text{CO}_2$. At a constant temperature, mean values of subsurface $f\text{CO}_2$ varied little from May to August (Fig. 12a). From August to October, however, temperature normalized $f\text{CO}_2$ (at 25 °C) in bottom waters increased by 300 μatm (Fig. 12a). This increase of

BGD

10, 3079–3120, 2013

Low pH and carbonate saturation state in the North Yellow Sea

W.-D. Zhai et al.

Title Page

Abstract

Introduction

Conclusions

References

Tables

Figures

⏪

⏩

◀

▶

Back

Close

Full Screen / Esc

Printer-friendly Version

Interactive Discussion



$f\text{CO}_2$ led to drops of 0.12 in pH_T (25 °C) and 0.40 in Ω_{arag} (in situ) from August to October (Fig. 12b, c).

4.3 Community respiration rate and its roles on the seasonal drops of subsurface pH and Ω_{arag}

At the same stations in June, August, and November, significant bottom water DO declines of 75 to 123 $\mu\text{mol O}_2 \text{ kg}^{-1}$ were determined from June to August in the southwestern and northern NYS areas under study (Fig. 13a), which were located around two high primary production cores (Fig. 5b) as indicated by the surface chl *a* values of 2.0–4.7 $\mu\text{g L}^{-1}$ observed in July. From August to November, bottom water DO declined again by 70 to 100 $\mu\text{mol O}_2 \text{ kg}^{-1}$ in the northwestern area (Fig. 13b). This highly DO depleted area was also located around the highest primary production core (Fig. 5c) as indicated by the surface chl *a* values of 4–11 $\mu\text{g L}^{-1}$ observed in October. Although changes in bottom water DO were subject to notable disturbance from horizontal transport and even vertical mixing, it was reasonable to conclude that the primary production indicated by the chl *a* results formed sufficient biogenic sinking particles, supporting notable respiration/remineralization in the bottom waters to consume bottom water DO. It was also reasonable to deduce that this DO consuming process (Eq. 1) led to a substantial addition of $f\text{CO}_2$ (Fig. 12a) and the seasonal drops in subsurface pH and Ω_{arag} (Fig. 12b, c). Similar to the pH-DO correlation cases in the northern Gulf of Mexico, and the northwestern East China Sea off the Changjiang Estuary, and the northwestern-northern Bohai Sea (Cai et al., 2011; Zhai et al., 2012), a positive correlation between subsurface DO and pH (25 °C) was also observed in the NYS (plots not reported), although it was biased in August and November by the water mixing process (see Sect. 4.4).

To estimate community respiration rates in the NYS bottom waters, we plotted bottom water DO concentrations versus salinity for deep stations in June, August, and November (Fig. 14a–c). In the NYS bottom water mass with typical salinity of 31.5–32.5 psu, the DO declined from 273–305 $\mu\text{mol O}_2 \text{ kg}^{-1}$ (average 292 $\mu\text{mol O}_2 \text{ kg}^{-1}$) in June to

Low pH and carbonate saturation state in the North Yellow Sea

W.-D. Zhai et al.

Title Page

Abstract

Introduction

Conclusions

References

Tables

Figures

⏪

⏩

◀

▶

Back

Close

Full Screen / Esc

Printer-friendly Version

Interactive Discussion



Low pH and carbonate saturation state in the North Yellow Sea

W.-D. Zhai et al.

[Title Page](#)

[Abstract](#)

[Introduction](#)

[Conclusions](#)

[References](#)

[Tables](#)

[Figures](#)

[⏪](#)

[⏩](#)

[◀](#)

[▶](#)

[Back](#)

[Close](#)

[Full Screen / Esc](#)

[Printer-friendly Version](#)

[Interactive Discussion](#)



229–263 $\mu\text{mol O}_2 \text{ kg}^{-1}$ (average 245 $\mu\text{mol O}_2 \text{ kg}^{-1}$) in August to 136–244 $\mu\text{mol O}_2 \text{ kg}^{-1}$ (average 193 $\mu\text{mol O}_2 \text{ kg}^{-1}$) in November (Fig. 14a–c). Since water stratification occurred in the summer months (Fig. 3), we can reasonably assume that possible DO recovery via vertical mixing was negligible. Therefore, this apparent DO depletion rate can be regarded as a rough estimate of the community respiration rate in the NYS bottom water mass, i.e. 0.8 $\mu\text{mol O}_2 \text{ kg}^{-1} \text{ d}^{-1}$ from June to August. This value was lower than the DO depletion rates of 2.0–2.8 $\mu\text{mol O}_2 \text{ kg}^{-1} \text{ d}^{-1}$ observed in the summer oxygen-depleted bottom water mass in the northwestern-northern Bohai Sea (Zhai et al., 2012).

From August to November, vertical mixing was enhanced (Fig. 3), resulting in DO recovery in many sampling sites. Even under strong disturbance, however, bottom water DO at seven selected sampling sites (from eleven stations with bottom water salinity of > 31.5) declined again by 50–90 $\mu\text{mol O}_2 \text{ kg}^{-1}$ in the NYS water mass (Fig. 14c), indicating August–November DO depletion rates in the NYS bottom water mass were 0.55–1.0 $\mu\text{mol O}_2 \text{ kg}^{-1} \text{ d}^{-1}$. This range was quite similar to the typical NYS bottom water DO depletion rate from June to August.

Figure 13 also shows the distributions of differences in bottom water pH_T (in situ) and Ω_{arag} in June, August, and November. These distributions reflect a synthesis effect of all regional/local processes on seasonal variations of subsurface pH and Ω_{arag} . Despite potential disturbances of water mixing, Fig. 13c–f present similar patterns to the apparent DO declines (Fig. 13a, b). From June to August, the great declines in pH_T (in situ) (0.20–0.26 pH units) and Ω_{arag} (0.30–0.43) occurred in the southwestern near-shore bottom waters (Fig. 13c, e). From August to November, however, another pH_T (in situ) reduction of 0.20 units and the greatest Ω_{arag} decrease of 0.60–0.62 were revealed in the northwestern near-shore bottom waters (Fig. 13d, f). If combined with distributions of bottom water pH_T and Ω_{arag} (Figs. 8, 10), the northwestern zone may represent the most vulnerable area in the NYS in terms of ocean acidification.

4.4 Effects of Bohai Sea water mass outflow

Figure 12c suggests that seasonal variation in air-equilibrated Ω_{arag} was also remarkable. With lowest salinity in August (Table 1), the air-equilibrated Ω_{arag} reached its highest peak (Fig. 12c) due to the outflow of the above-mentioned low-salinity/high-NTalk Bohai Sea water mass.

To examine effects of the Bohai Sea water mass outflow, bottom water Ω_{arag} at deep stations in the NYS were plotted against salinity (Fig. 15a–g). In all these surveys, bottom water Ω_{arag} declined with salinity increase. In the typical Bohai Sea water salinity range of 30.5–31.5 psu, the bottom water Ω_{arag} ranged between 1.6 and 2.4 (Fig. 15a–g), although very low values of 1.3–1.4 with salinity of 30.5–31.5 psu were also revealed at three stations in October and at one station in November (Fig. 15e, f). In the typical NYS water salinity range of 31.5–32.5 psu, however, low Ω_{arag} values of < 1.6 were frequently observed during every survey. Even in October, most bottom water Ω_{arag} values were in the critically low range of 1.0–1.2 at nine out of thirteen deep stations with salinity of > 31.5 psu (Fig. 15e).

Similarly, bottom water pH_T (25 °C) in general declined with salinity increase (Fig. 14d–g). In the salinity range of 30.5–31.5 psu, the bottom water pH_T (25 °C) ranged mostly between 7.76 and 7.94 (Fig. 14d–g). In the typical NYS water salinity range of 31.5–32.5 psu, however, low bottom water pH_T (25 °C) values of < 7.70 were frequently observed during most surveys. In October, all bottom water pH_T values (25 °C) with salinity of > 31.5 psu were observed at very low values of 7.53 to 7.66 (Fig. 14f).

In the southwestern part of the NYS, the Bohai Sea water mass influenced bottom waters, as indicated by low salinity (Fig. 4) and high NTalk (Fig. 9). The high pH_T (25 °C) (Fig. 8) and high Ω_{arag} (Fig. 10) characteristics of this water mass were consistent with previously reported insignificant bottom water DO depletion/pH decline in the south-eastern Bohai Sea in summer months (Zhai et al., 2012). Therefore, the Bohai Sea water mass outflow had important impacts on the dynamics of subsurface pH (25 °C)

BGD

10, 3079–3120, 2013

Low pH and carbonate saturation state in the North Yellow Sea

W.-D. Zhai et al.

Title Page

Abstract

Introduction

Conclusions

References

Tables

Figures

⏪

⏩

◀

▶

Back

Close

Full Screen / Esc

Printer-friendly Version

Interactive Discussion

and Ω_{arag} in the NYS (Figs. 8, 10). In the most acidified month of October, Bohai Sea water mass outflow effectively increased the NYS mean bottom water Ω_{arag} by 0.28 (Fig. 12c), although its effects on pH (in situ) were counteracted with the temperature effect (Fig. 12b). Figure 15h eliminates the influences of $f\text{CO}_2$ on bottom water Ω_{arag} , suggesting that the seasonal effect of the Bohai Sea water mass outflow on bottom water Ω_{arag} accounted for a variation of 0.54, which was larger than the overall seasonal variation of 0.45 in bottom water Ω_{arag} in 2011 (Fig. 12c).

4.5 Recent regional environmental changes and their potential impacts

The high frequency of red tides in the past 30 yr indicates eutrophication in the NYS (Zhang, 1994; State Oceanic Administration of China, <http://www.mem.gov.cn/gjgb/index.htm>). In June 2011, however, surface water nutrients in the NYS were measured at low concentrations of $0.5\text{--}1.2\ \mu\text{mol L}^{-1}$ for DIN (nitrate + nitrite + ammonium), $<0.03\ \mu\text{mol L}^{-1}$ for phosphate, and $1.0\text{--}5.0\ \mu\text{mol L}^{-1}$ for dissolved silicate (Zhai et al., unpublished data), which were similar to values obtained in the early 1990s (Zhang, 1994). According to Zhang (1994), atmospheric deposition of nutrient elements and trace species causes red tides to develop in this region. Based on a synthesis research, Bashkin et al. (2002) concluded that typical annual nitrogen input into the Yellow Sea in the late 1990s was approximately $2.6 \times 10^{12}\ \text{g N}$. Annual accumulation of N in the Yellow Sea was estimated at approximately $1.2 \times 10^{12}\ \text{g N}$, with a residence time for nitrogen of about 1.5 yr (Bashkin et al., 2002). The majority of this nitrogen loading was human-derived, which led to excessive water eutrophication in the Yellow Sea.

On the other hand, annual water discharge of the lower Yellow River has significantly declined during the past 50 yr from mostly $(30\text{--}70) \times 10^9\ \text{m}^3\ \text{yr}^{-1}$ in the 1950s and 1960s to $\sim 5 \times 10^9\ \text{m}^3\ \text{yr}^{-1}$ in the late 1990s (Wu et al., 2004; Wang et al., 2007; Fig. 2b), and leading to a salinity increase in the Bohai Sea by 2 psu (Wu et al., 2004; Ning et al., 2010). Although water flux from the Yellow River estuary into the Bohai Sea increased again to $\sim 20 \times 10^9\ \text{m}^3\ \text{yr}^{-1}$ over the last ten years (Fig. 2b) due to human manipulation of water discharge, the material flux and alkalinity export of the lower Yellow

BGD

10, 3079–3120, 2013

Low pH and carbonate saturation state in the North Yellow Sea

W.-D. Zhai et al.

Title Page

Abstract

Introduction

Conclusions

References

Tables

Figures

⏪

⏩

◀

▶

Back

Close

Full Screen / Esc

Printer-friendly Version

Interactive Discussion

Low pH and carbonate saturation state in the North Yellow Sea

W.-D. Zhai et al.

Title Page

Abstract

Introduction

Conclusions

References

Tables

Figures

⏪

⏩

◀

▶

Back

Close

Full Screen / Esc

Printer-friendly Version

Interactive Discussion

River only account for 30%–66% of those values in the 1950s and 1960s. The reduced water discharge still supports the significant Bohai Sea water mass outflow and thereby an alkalinity source in the NYS, as indicated by the NYS mean bottom water salinity drop in August (Table 1) and the NYS bottom water NTalk distributions (Fig. 9).

In the hydrological settings during the 1950s and 1960s, more Bohai Sea water and TAlk were introduced into the NYS, and the above-mentioned seasonal acidification processes were mitigated much more than present. Therefore, the recent occurrence of low Ω_{arag} status in the NYS subsurface waters is not only influenced by global atmospheric CO_2 increase and local respiration/remineralization (Feely et al., 2010; Cai et al., 2011; Sunda and Cai, 2012), but also by major environmental changes in the regional system of the Yellow River – Bohai Sea – North Yellow Sea. This issue requires further investigation.

5 Summary and implications

In summary, we investigated the dynamics of subsurface pH and Ω_{arag} in 2011 on the Chinese side of the North Yellow Sea. Our results indicate that this western North Pacific continental margin was substantially influenced by global atmospheric CO_2 increase. Local community respiration/remineralization led to seasonal drops in subsurface pH and Ω_{arag} , although outflow of the Bohai Sea water mass counteracted the subsurface Ω_{arag} reduction in the warm seasons. Very low pH_T values (25°C) of 7.53–7.60 and critically low Ω_{arag} values of 1.0–1.2 were revealed in subsurface waters in October in ~10% of the North Yellow Sea area. In areas with extremely low pH and Ω_{arag} , carbonate biominerals in calcic shells and skeletons may begin to significantly dissolve. This status may seriously injure the adjacent marine aquaculture zones, which are of major economic importance in North China.

In a broader context, coastal ocean acidification is influenced by the combined effect of many contributors, including global atmospheric CO_2 increases and regional/local forcings (Feely et al., 2010; Kelly et al., 2011; Gruber et al., 2012). The North Yellow

Sea is clearly one of these complex regimes. Moreover, this study presents a unique example of regional environment changes resulting from elevated nutrient discharges from land and reduction in terrestrial alkalinity inputs on coastal ocean acidification.

Appendix A

5 Comparison between parallel pH measurements

Based on parallel measurements in June and November using two pH buffer sets, we concluded that the pH data on the total-hydrogen-ion scale were lower than the NIST-traceable pH data by 0.143 ± 0.003 pH units (mean \pm standard deviation, $n = 62$, based on the experiment in June) in the North Yellow Sea (Fig. A1).

10 Appendix B

Comparison between measured and calculated dissolved inorganic carbon

By comparison with field measured dissolved inorganic carbon (DIC) data in June, August, and November (Zhai et al., unpublished data), most relative deviations of calculated DIC were at a satisfactory level of less than 1 % (Fig. A2).

15 *Acknowledgements.* We thank Liguó Guo, Xiao Huang, Di Qi, and Ying Wang for the collection of ancillary data, Deli Wang for his constructive discussion, and Christine Watts for her assistance with English. Houjie Wang, Xiao Huang, Yuwen Jiang, Minghao Li and the crews of R/V *Dongfanghong II* and R/V *Yixing* provided much help during the sampling surveys. The research was supported by the National Basic Research Program of China (2009CB421204) and the National Natural Science Foundation of China (NSFC) (41276061 and 41076044).
20 Sampling surveys were jointly supported by the pilot project of the State Oceanic Administration of China (SOA) on air-sea carbon dioxide flux monitoring in the North Yellow Sea, the NSFC (41049901 and 40876040), and the SOA (contract DOMEF-MEA-01-10).

Low pH and carbonate saturation state in the North Yellow Sea

W.-D. Zhai et al.

Title Page

Abstract

Introduction

Conclusions

References

Tables

Figures

⏪

⏩

◀

▶

Back

Close

Full Screen / Esc

Printer-friendly Version

Interactive Discussion



References

- Bashkin, V. N., Park, S. U., Choi, M. S., and Lee, C. B.: Nitrogen budgets for the Republic of Korea and the Yellow Sea region, *Biogeochemistry*, 57/58, 387–403, 2002.
- Baumann, H., Talmage, S. C., and Gobler, C. J.: Reduced early life growth and survival in a fish in direct response to increased carbon dioxide, *Nat. Clim. Chang.*, 2, 38–41, 2012.
- Benson, B. B. and Krause, D.: The concentration and isotopic fractionation of oxygen dissolved in fresh water and seawater in equilibrium with the atmosphere, *Limnol. Oceanogr.*, 29, 620–632, 1984.
- Cai, W.-J., Hu, X.-P., Huang, W.-J., Murrell, M.-C., Lehrter, J. C., Lohrenz, S. E., Chou, W.-C., Zhai W.-D., Hollibaugh, J. T., Wang, Y.-C., Zhao, P.-S., Guo, X.-H., Gundersen, K., Dai, M.-H., and Gong, G.-C.: Acidification of subsurface coastal waters enhanced by eutrophication, *Nat. Geosci.*, 4, 766–770, 2011.
- Chen, J.-S., Wang, F.-Y., Meybeck, M., He, D.-W., Xia, X.-H., and Zhang, L.-T.: Spatial and temporal analysis of water chemistry records (1958–2000) in the Huanghe (Yellow River) basin, *Global Biogeochem. Cy.*, 19, GB3016, doi:10.1029/2004GB002325, 2005.
- Dickson, A. G.: Standard potential of the reaction: $\text{AgCl(s)} + 1/2 \text{H}_2(\text{g}) = \text{Ag(s)} + \text{HCl(aq)}$, and the standard acidity constant of the ion HSO_4^- in synthetic sea water from 273.15 to 318.15 K, *J. Chem. Thermodyn.*, 22, 113–127, 1990.
- Dickson, A. G., Sabine, C. L., and Christian, J. R.: Guide to Best Practices for Ocean CO_2 Measurements, *PICES Spec. Publ.*, no. 3, 2007.
- Domenici, P., Allan, B., McCormick, M. I., and Munday, P. L.: Elevated carbon dioxide affects behavioural lateralization in a coral reef fish, *Biol. Lett.*, 8, 78–81, 2012.
- Doney, S. C., Fabry, V. J., Feely, R. A., and Kleypas, J. A.: Ocean acidification: the other CO_2 problem, *Annu. Rev. Mar. Sci.*, 1, 169–192, 2009.
- Feely, R. A., Sabine, C. L., Lee, K., Millero, F. J., Lamb, M. F., Greeley, D., Bullister, J. L., Key, R. M., Peng, T.-H., Kozyr, A., Ono, T., and Wong, C. S.: In situ calcium carbonate dissolution in the Pacific Ocean, *Global Biogeochem. Cy.*, 16, 1144, doi:10.1029/2002GB001866, 2002.
- Feely, R. A., Alin, S. R., Newton, J., Sabine, S. L., Warner, M., Devol, A., Krembs, C., and Maloy, C.: The combined effects of ocean acidification, mixing, and respiration on pH and carbonate saturation in an urbanized estuary, *Estuar. Coast. Shelf S.*, 88, 442–449, 2010.

BGD

10, 3079–3120, 2013

Low pH and carbonate saturation state in the North Yellow Sea

W.-D. Zhai et al.

Title Page

Abstract

Introduction

Conclusions

References

Tables

Figures

⏪

⏩

◀

▶

Back

Close

Full Screen / Esc

Printer-friendly Version

Interactive Discussion

Low pH and carbonate saturation state in the North Yellow Sea

W.-D. Zhai et al.

[Title Page](#)

[Abstract](#)

[Introduction](#)

[Conclusions](#)

[References](#)

[Tables](#)

[Figures](#)



[Back](#)

[Close](#)

[Full Screen / Esc](#)

[Printer-friendly Version](#)

[Interactive Discussion](#)

- Feng, S.-Z., Zhang, J., and Wei, H.: Environmental Dynamics in the Bohai Sea, Science Press, Beijing, China, 281 pp., 2007 (in Chinese).
- Gao, K.-S., Aruga, Y., Asada, K., Ishihara, T., Akano, T., and Kiyohara, M.: Calcification in the articulated coralline alga *Carollina pilulifera*, with special reference to the effect of elevated CO₂ concentration, *Mar. Biol.*, 117, 129–132, 1993.
- Gieskes, J. M.: Effect of temperature on the pH of seawater, *Limnol. Oceanogr.*, 14, 679–685, 1969.
- Gruber, N., Hauri, C., Lachkar, Z., Loher, D., Frölicher, T. L., and Plattner, G. K.: Rapid progression of ocean acidification in the California current system, *Science*, 337, 220–223, 2012.
- Hall-Spencer, J. M., Rodolfo-Metalpa, R., Martin, S., Ransome, E., Fine, M., Turner, S. M., Rowley, S. J., Tedesco, D., and Buia, M. C.: Volcanic carbon dioxide vents show ecosystem effects of ocean acidification, *Nature*, 454, 96–99, 2008.
- Huang, B.-Q., Lan, W.-L., Cao, Z.-R., Dai, M.-H., Huang, L.-F., Jiao, N.-Z., and Hong, H.-S.: Spatial and temporal distribution of nanoflagellates in the northern South China Sea, *Hydrobiologia*, 605, 143–157, 2008.
- Lee, K., Tong, L. T., Millero, F. J., Sabine, C. L., Dickson, A. G., Goyet, C., Park, G. H., Wanninkhof, R., Feely, R. A., and Key, R. M.: Global relationships of total alkalinity with salinity and temperature in surface waters of the world's oceans, *Geophys. Res. Lett.*, 33, L19605, doi:10.1029/2006GL027207, 2006.
- Lewis, E., and Wallace, D. W. R.: Program Developed for CO₂ System Calculations, ORNL/CDIAC-105, Carbon Dioxide Information Analysis Center, Oak Ridge National Laboratory, US Department of Energy, Oak Ridge, Tennessee, 1998.
- Millero, F. J., Graham, T. B., Huang, F., Bustos-Serrano, H., and Pierrot, D.: Dissociation constants of carbonic acid in seawater as a function of salinity and temperature, *Mar. Chem.*, 100, 80–94, 2006.
- Mucci, A.: The solubility of calcite and aragonite in seawater at various salinities, temperatures, and one atmosphere total pressure, *Am. J. Sci.*, 283, 780–799, 1983.
- Munday, P. L., Dixon, D. L., Donelson, J. M., Jones, G. P., Pratchett, M. S., Devitsina, G. V., and Døving, K. B.: Ocean acidification impairs olfactory discrimination and homing ability of a marine fish, *P. Natl. Acad. Sci. USA*, 106, 1848–1852, 2009.
- Munday, P. L., Dixon, D. L., McCormick, M. I., Meekan, M., Ferraric, M. C. O., and Chivers, D. P.: Replenishment of fish populations is threatened by ocean acidification, *P. Natl. Acad. Sci. USA*, 107, 12930–12934, 2010.

Low pH and carbonate saturation state in the North Yellow Sea

W.-D. Zhai et al.

[Title Page](#)

[Abstract](#)

[Introduction](#)

[Conclusions](#)

[References](#)

[Tables](#)

[Figures](#)

[⏪](#)

[⏩](#)

[◀](#)

[▶](#)

[Back](#)

[Close](#)

[Full Screen / Esc](#)

[Printer-friendly Version](#)

[Interactive Discussion](#)



- Ning, X.-R., Lin, C.-L., Su, J.-L., Liu, C.-G., Hao, Q., Le, F.-F., and Tang, Q.-S.: Long-term environmental changes and the responses of the ecosystems in the Bohai Sea during 1960–1996, *Deep-Sea Res. Pt. II*, 57, 1079–1091, 2010.
- Parsons, T. R., Yoshiaki, M., and Lalli, C. M.: *A Manual of Chemical and Biological Methods for Seawater Analysis*, Pergamon Press, Oxford, 1984.
- Pelletier, G. J., Lewis, E., and Wallace, D. W. R.: *CO2SYS.XLS: a Calculator for the CO₂ System in Seawater for Microsoft Excel/VBA, Version 16*, Washington State Department of Ecology, Olympia, Washington, 2011.
- Sunda, W. G., and Cai, W.-J.: Eutrophication induced CO₂-acidification of subsurface coastal waters: interactive effects of temperature, salinity, and atmospheric $p\text{CO}_2$, *Environ. Sci. Technol.*, 46, 10651–10659, 2012.
- Wang, H.-J., Yang, Z.-S., Saito, Y., Liu, J.-P., Sun, X.-X., and Wang, Y.: Stepwise decreases of the Huanghe (Yellow River) sediment load (1950–2005): impacts of climate change and human activities, *Global Planet. Change*, 57, 331–354, 2007.
- Wang, X.-L., Zhang, L.-J., Su, Z., Li, Y., Zhang, X.-S., and Gao, H.-W.: The conservative and non-conservative behavior of total alkalinity in the Huanghe estuary, *J. Ocean Univ. China*, 35, 1063–1066, 2005 (in Chinese).
- Wang, Y.-C., Liu, Z., Gao, H.-W., Ju, L., and Guo, X.-Y.: Response of salinity distribution around the Yellow River mouth to abrupt changes in river discharge, *Cont. Shelf Res.*, 31, 685–694, 2011.
- WMO/GAW: The state of greenhouse gases in the atmosphere based on global observations through 2011, *WMO Greenhouse Gas Bull.*, no. 8, 1–4, 2012.
- Wong, G. T. F.: Removal of nitrite interference in the Winkler determination of dissolved oxygen in seawater, *Mar. Chem.*, 130/131, 28–32, 2012.
- Wu, D.-X., Mu, L., Li, Q., Bao, X.-W., and Wan, X.-Q.: Characteristics of long-term variations of sea water salinity in the Bohai Sea and the possible controls, *Prog. Nat. Sci.*, 14, 191–195, 2004 (in Chinese).
- Yuan, Y.-X., Chen, J.-F., Chen, B.-J., Qu, K.-M., Guo, F., Li, Q.-F., and Cui, Y.: Study on adaptability of scallop *Chlamys farreri* to environment: effects of salinity and pH on survival, respiration, ingestion and digestion, *J. Fish Sci. China*, 7, 73–77, 2000 (in Chinese).
- Zeebe, R. E., Zachos, J. C., Caldeira, K., and Tyrrell, T.: Carbon emissions and acidification, *Science*, 321, 51–52, 2008.

Zhai, W.-D., Zhao, H.-D., Zheng, N., and Xu, Y.: Coastal acidification in summer bottom oxygen-depleted waters in northwestern-northern Bohai Sea from June to August in 2011, *Chin. Sci. Bull.*, 57, 1062–1068, 2012.

Zhang, J.: Atmospheric wet deposition of nutrient elements: correlation with harmful biological blooms in Northwest Pacific coastal zones, *Ambio*, 23, 464–468, 1994.

5

BGD

10, 3079–3120, 2013

Low pH and carbonate saturation state in the North Yellow Sea

W.-D. Zhai et al.

Title Page

Abstract

Introduction

Conclusions

References

Tables

Figures



Back

Close

Full Screen / Esc

Printer-friendly Version

Interactive Discussion



Low pH and carbonate saturation state in the North Yellow Sea

W.-D. Zhai et al.

Table 1. Cruise summary and typical temperature, salinity, TALK, pH_T , DO, and calculated Ω_{arag} in bottom waters at deep stations (water depth > 25 m). Data were summarized using mean \pm standard deviation.

Surveying dates	Deep stations	Temperature ($^{\circ}\text{C}$)	Salinity (psu)	TALK ($\mu\text{mol kg}^{-1}$)	pH_T (25°C)	DO ($\mu\text{mol O}_2 \text{ kg}^{-1}$)	Ω_{arag}
10–17 May 2011	21	5.5 ± 1.3	31.89 ± 0.33	2287 ± 25	7.79 ± 0.05	no data	1.74 ± 0.17
22–24 Jun 2011	14	7.0 ± 2.5	31.88 ± 0.22	2293 ± 12	7.79 ± 0.07	291 ± 12	1.77 ± 0.26
24–31 Jul 2011	19	9.3 ± 3.4	31.80 ± 0.33	2282 ± 15	7.77 ± 0.07	no data	1.70 ± 0.26
20–26 Aug 2011	13	13.3 ± 5.0	31.36 ± 0.59	2262 ± 39	7.77 ± 0.09	227 ± 24	1.72 ± 0.33
18–23 Oct 2011	19	11.8 ± 3.5	31.55 ± 0.49	2254 ± 34	7.65 ± 0.10	no data	1.32 ± 0.31
22–25 Nov 2011	19	11.2 ± 2.1	31.55 ± 0.51	2245 ± 31	7.72 ± 0.10	208 ± 33	1.50 ± 0.28
09–13 Jan 2012	6	6.0 ± 0.6	31.74 ± 0.39	2237 ± 18	7.71 ± 0.05	302 ± 9	1.41 ± 0.12

Title Page

Abstract

Introduction

Conclusions

References

Tables

Figures



Back

Close

Full Screen / Esc

Printer-friendly Version

Interactive Discussion

Low pH and carbonate saturation state in the North Yellow Sea

W.-D. Zhai et al.

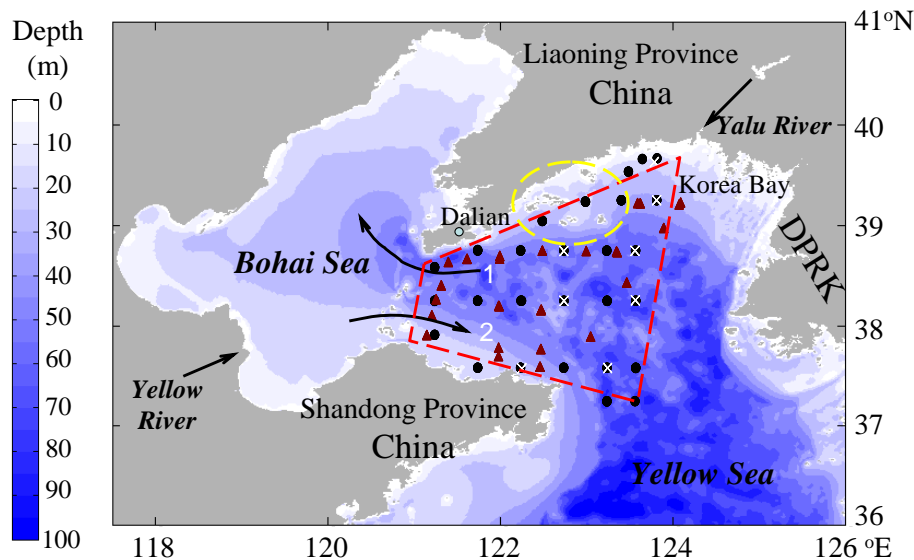


Fig. 1. Area map and sampling sites. Closed circles were sampled in May, July, and October. Triangles were sampled in June, August, and November. White crosses were sampled in January 2012. The study area is enclosed with the red-line polygon. A major marine aquaculture zone is enclosed with the yellow-line ellipse. The Bohai Sea inflow current (1) and Bohai Sea outflow current (2) are based on Feng et al. (2007).

Title Page

Abstract

Introduction

Conclusions

References

Tables

Figures

◀

▶

◀

▶

Back

Close

Full Screen / Esc

Printer-friendly Version

Interactive Discussion

Low pH and carbonate saturation state in the North Yellow Sea

W.-D. Zhai et al.

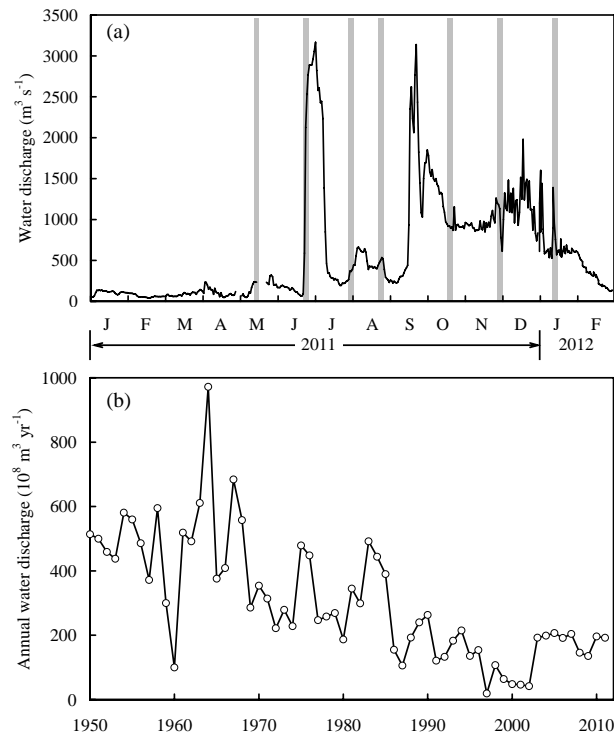
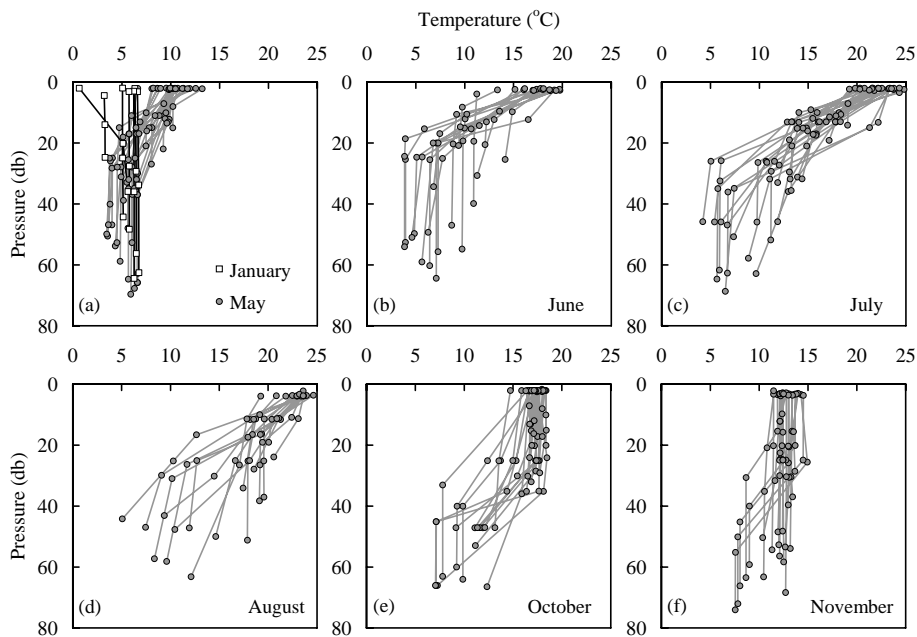


Fig. 2. Evolutions of water discharge from the Yellow River emptying into the Bohai Sea from January 2011 to February 2012 **(a)**, and from 1950 to 2011 **(b)**. Annual data of 1950–2005 were from Wang et al. (2007), while real time data of 2006–2012 were weekly downloaded from website of China Bureau of Hydrology (<http://xxfb.hydroinfo.gov.cn/>). Vertical grey columns in **(a)** show surveying dates.

[Title Page](#)[Abstract](#)[Introduction](#)[Conclusions](#)[References](#)[Tables](#)[Figures](#)[◀](#)[▶](#)[◀](#)[▶](#)[Back](#)[Close](#)[Full Screen / Esc](#)[Printer-friendly Version](#)[Interactive Discussion](#)

Low pH and carbonate saturation state in the North Yellow Sea

W.-D. Zhai et al.

**Fig. 3.** Depth profiles of water temperature.[Title Page](#)[Abstract](#)[Introduction](#)[Conclusions](#)[References](#)[Tables](#)[Figures](#)[◀](#)[▶](#)[◀](#)[▶](#)[Back](#)[Close](#)[Full Screen / Esc](#)[Printer-friendly Version](#)[Interactive Discussion](#)

Low pH and carbonate saturation state in the North Yellow Sea

W.-D. Zhai et al.

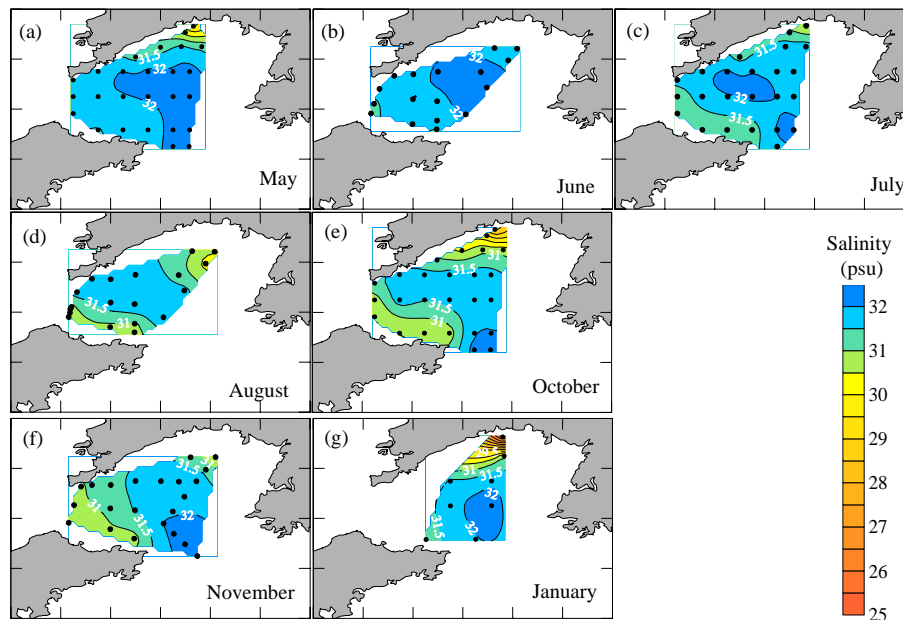


Fig. 4. Distributions of salinity in bottom waters.

[Title Page](#)

[Abstract](#)

[Introduction](#)

[Conclusions](#)

[References](#)

[Tables](#)

[Figures](#)



[Back](#)

[Close](#)

[Full Screen / Esc](#)

[Printer-friendly Version](#)

[Interactive Discussion](#)

Low pH and
carbonate saturation
state in the North
Yellow Sea

W.-D. Zhai et al.

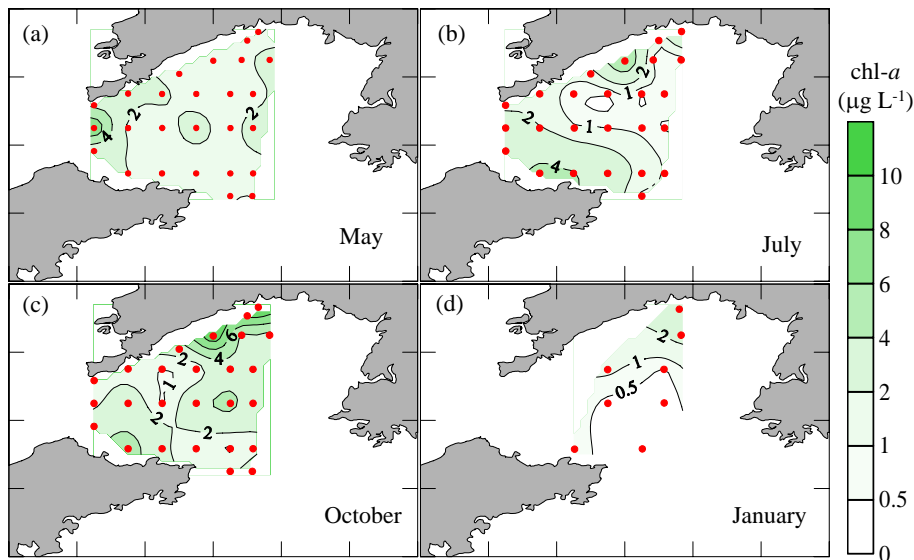
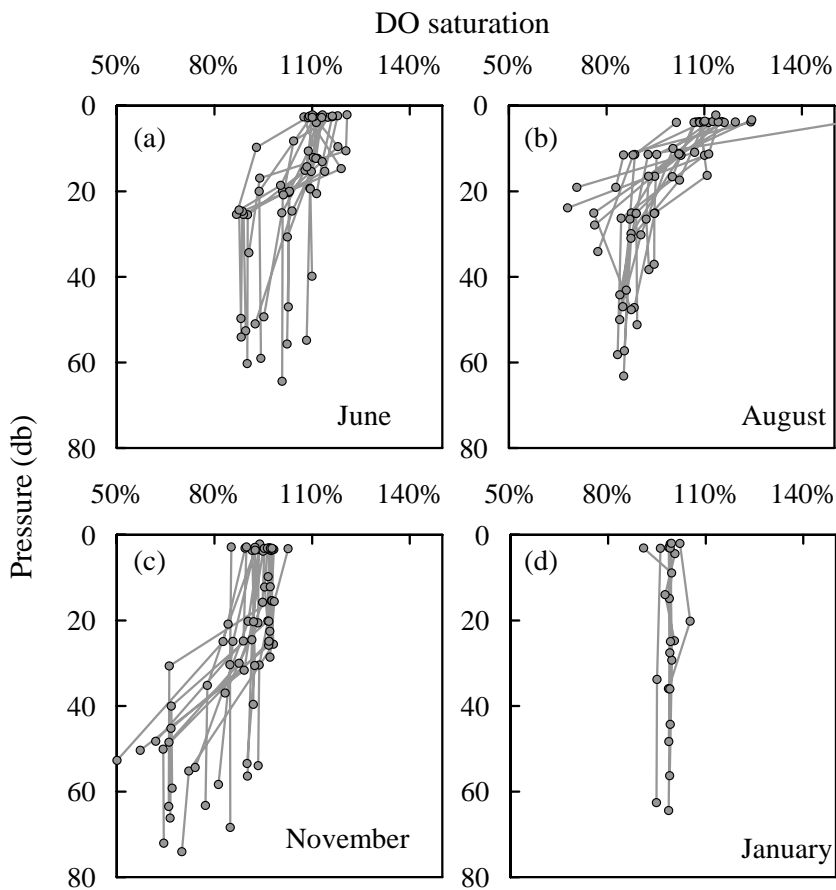


Fig. 5. Distributions of sea surface chlorophyll *a* (chl *a*) concentrations.

[Title Page](#)[Abstract](#)[Introduction](#)[Conclusions](#)[References](#)[Tables](#)[Figures](#)[⏪](#)[⏩](#)[◀](#)[▶](#)[Back](#)[Close](#)[Full Screen / Esc](#)[Printer-friendly Version](#)[Interactive Discussion](#)

Low pH and carbonate saturation state in the North Yellow Sea

W.-D. Zhai et al.

**Fig. 6.** Depth profiles of dissolved oxygen (DO) saturation.[Title Page](#)[Abstract](#)[Introduction](#)[Conclusions](#)[References](#)[Tables](#)[Figures](#)[◀](#)[▶](#)[◀](#)[▶](#)[Back](#)[Close](#)[Full Screen / Esc](#)[Printer-friendly Version](#)[Interactive Discussion](#)

Low pH and carbonate saturation state in the North Yellow Sea

W.-D. Zhai et al.

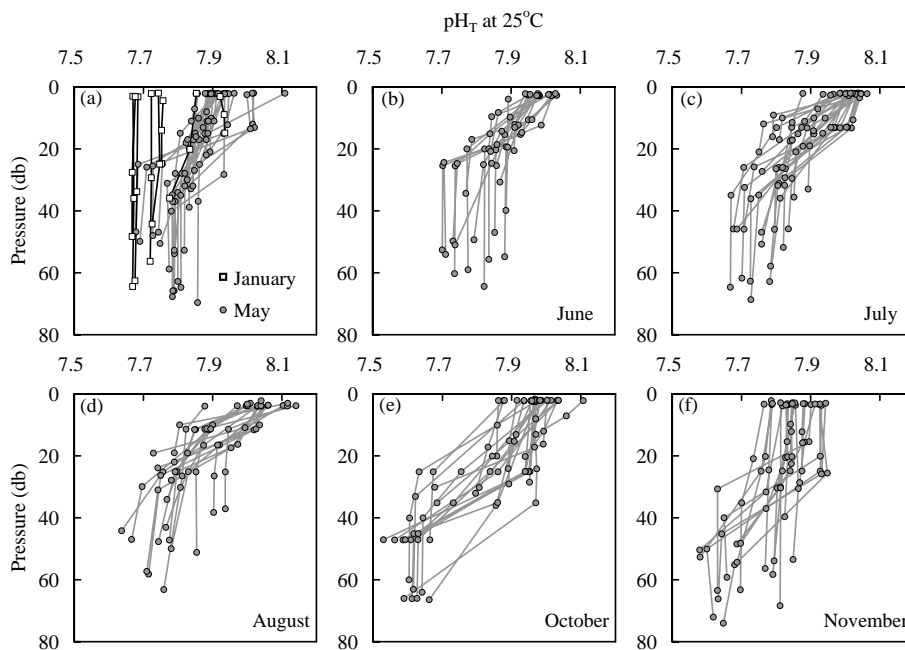


Fig. 7. Depth profiles of pH_T (25°C).

Title Page

Abstract

Introduction

Conclusions

References

Tables

Figures

◀

▶

◀

▶

Back

Close

Full Screen / Esc

Printer-friendly Version

Interactive Discussion

Low pH and carbonate saturation state in the North Yellow Sea

W.-D. Zhai et al.

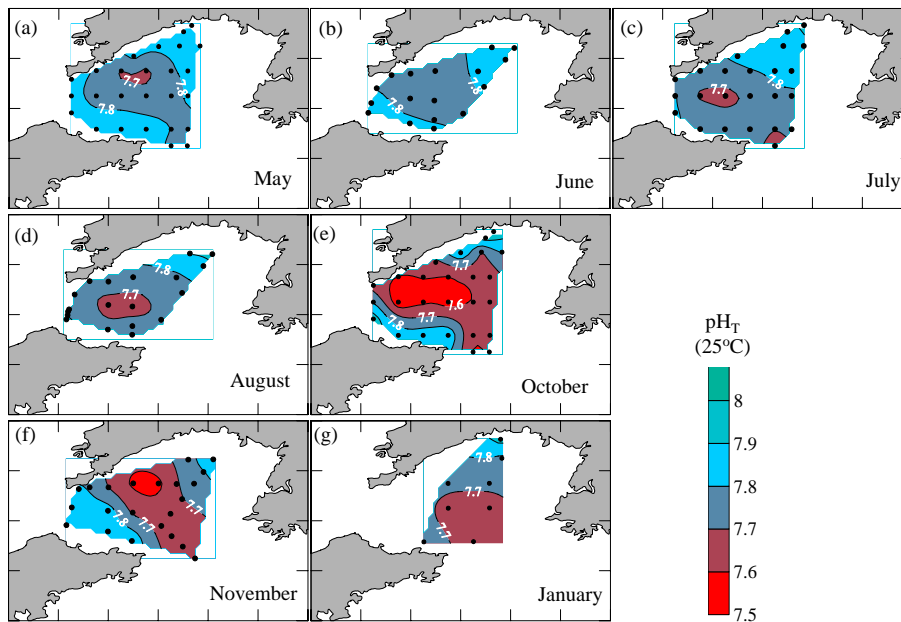


Fig. 8. Distributions of pH_T (25°C) in bottom waters.

Title Page

Abstract

Introduction

Conclusions

References

Tables

Figures

◀

▶

◀

▶

Back

Close

Full Screen / Esc

Printer-friendly Version

Interactive Discussion

Low pH and carbonate saturation state in the North Yellow Sea

W.-D. Zhai et al.

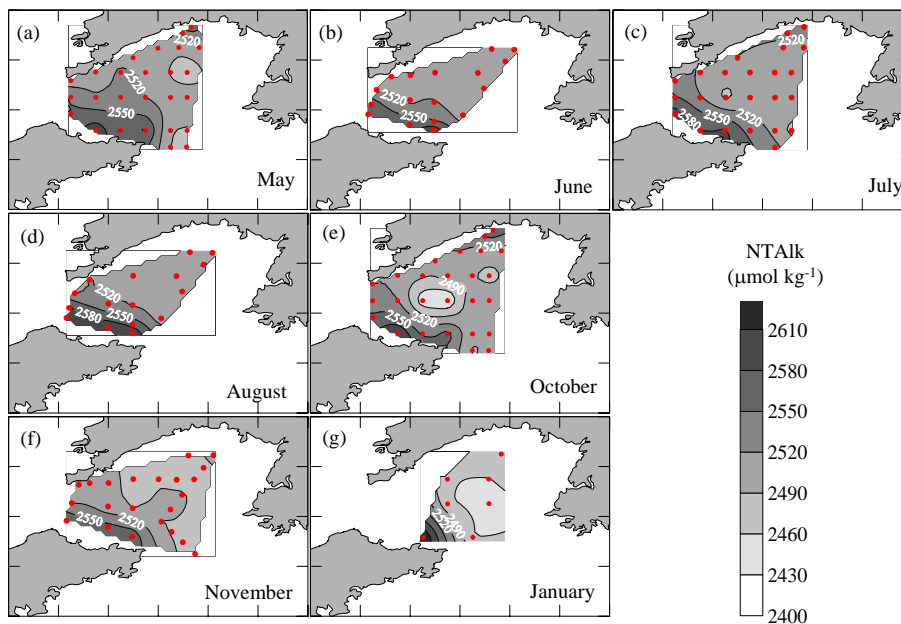


Fig. 9. Distributions of salinity normalized total alkalinity (NTAlk) in bottom waters.

Title Page

Abstract

Introduction

Conclusions

References

Tables

Figures

⏪

⏩

◀

▶

Back

Close

Full Screen / Esc

Printer-friendly Version

Interactive Discussion

Low pH and carbonate saturation state in the North Yellow Sea

W.-D. Zhai et al.

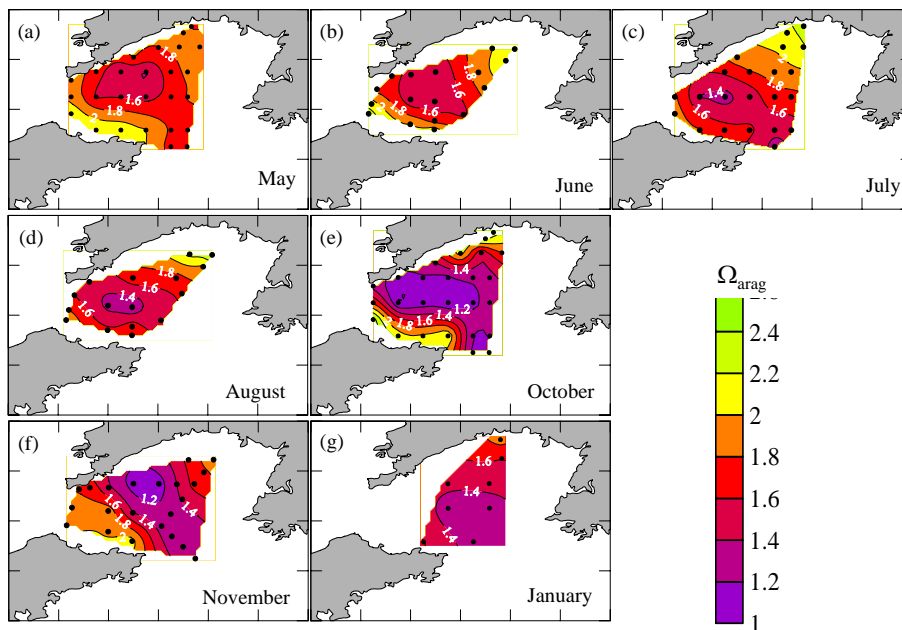


Fig. 10. Distributions of carbonate saturation state of aragonite (Ω_{arag}) in bottom waters.

Title Page

Abstract

Introduction

Conclusions

References

Tables

Figures

⏪

⏩

◀

▶

Back

Close

Full Screen / Esc

Printer-friendly Version

Interactive Discussion

Low pH and carbonate saturation state in the North Yellow Sea

W.-D. Zhai et al.

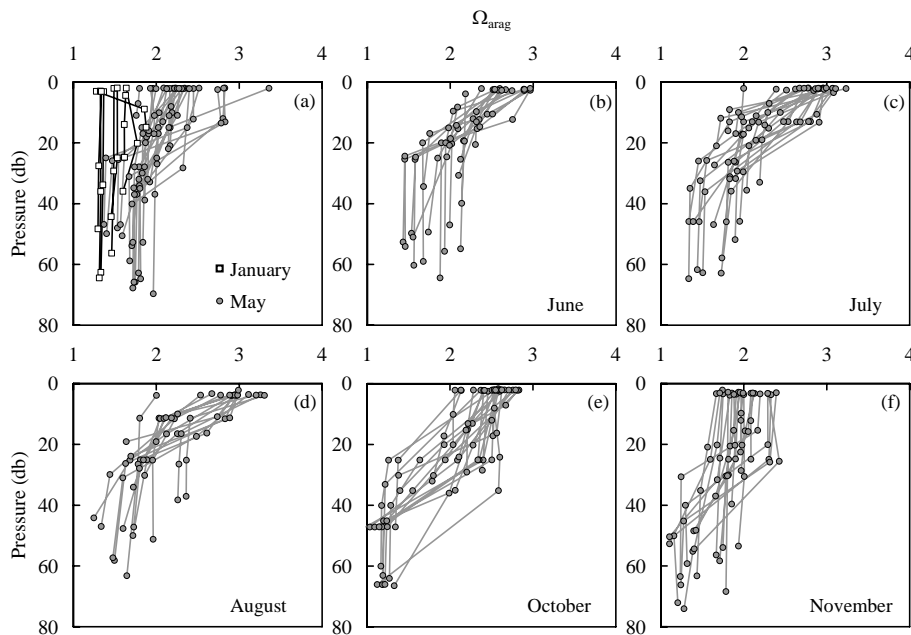


Fig. 11. Depth profiles of carbonate saturation state of aragonite (Ω_{arag}).

Title Page

Abstract

Introduction

Conclusions

References

Tables

Figures

◀

▶

◀

▶

Back

Close

Full Screen / Esc

Printer-friendly Version

Interactive Discussion

Low pH and carbonate saturation state in the North Yellow Sea

W.-D. Zhai et al.

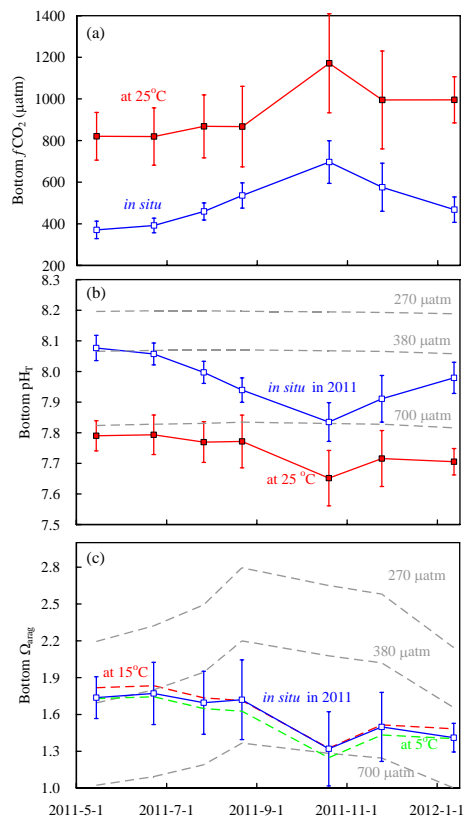


Fig. 12. Time series of survey average values of bottom water CO_2 fugacity ($f\text{CO}_2$) **(a)**, pH_T **(b)**, and carbonate saturation state of aragonite (Ω_{arag}) **(c)** at deep stations (water depth > 25 m). Colored points and lines show data at different temperature. Error bars mean standard deviation. Grey dashed lines in panels **(b)** and **(c)** mean modeled data under averaged bottom water temperature, salinity, TALK (Table 1), and different $f\text{CO}_2$ levels.

Title Page

Abstract

Introduction

Conclusions

References

Tables

Figures

◀

▶

◀

▶

Back

Close

Full Screen / Esc

Printer-friendly Version

Interactive Discussion

Low pH and carbonate saturation state in the North Yellow Sea

W.-D. Zhai et al.

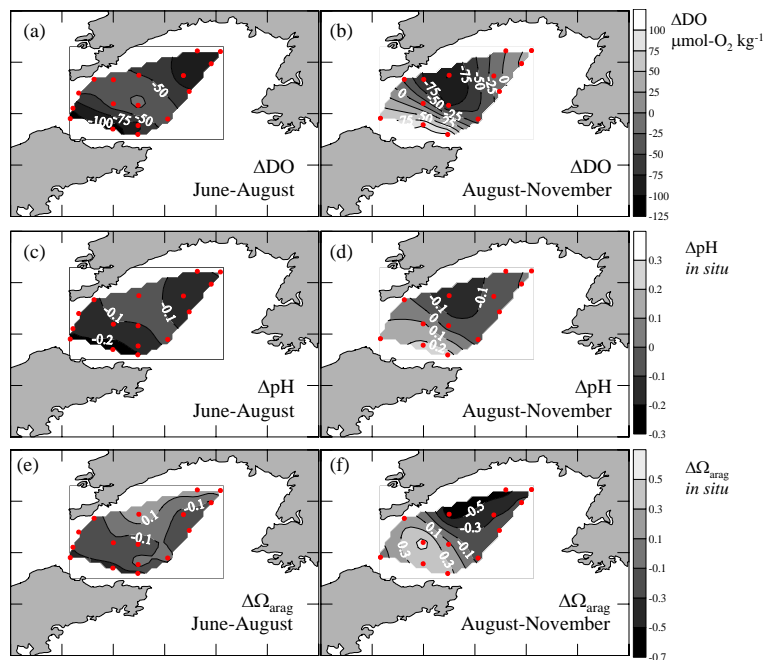


Fig. 13. Distributions of differences in bottom water DO (**a, b**), differences in bottom water pH_T (in situ) (**c, d**), and differences in bottom water carbonate saturation state of aragonite (Ω_{arag}) (**e, f**) in June, August, and November.

Title Page

Abstract

Introduction

Conclusions

References

Tables

Figures

⏪

⏩

◀

▶

Back

Close

Full Screen / Esc

Printer-friendly Version

Interactive Discussion

Low pH and carbonate saturation state in the North Yellow Sea

W.-D. Zhai et al.

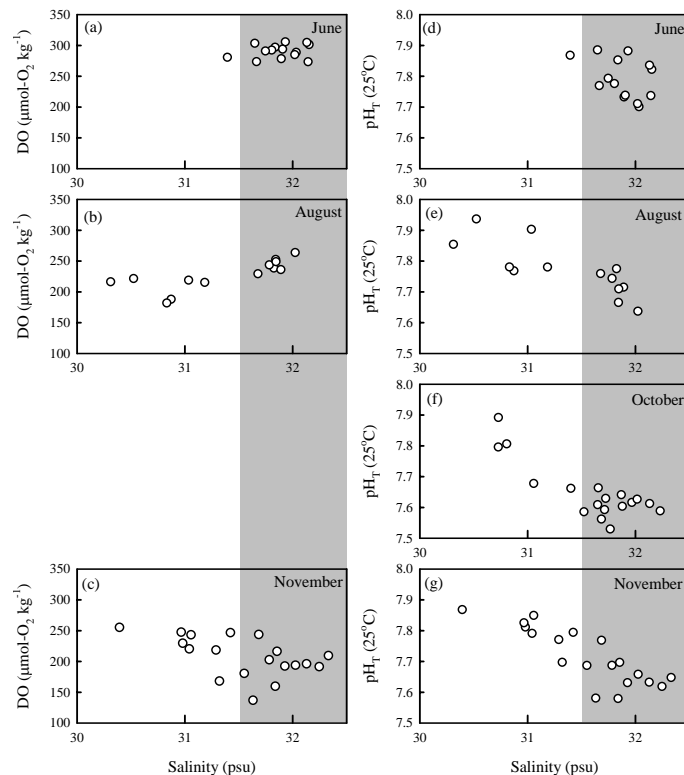


Fig. 14. Bottom water dissolved oxygen (DO) concentrations versus salinity (a–c), and bottom water pH_T (25°C) versus salinity (d–g) at deep stations (water depth > 25 m) in June, August, October, and November. The typical NYS salinity range of 31.5–32.5 is shadowed.

[Title Page](#)
[Abstract](#)
[Introduction](#)
[Conclusions](#)
[References](#)
[Tables](#)
[Figures](#)
[⏪](#)
[⏩](#)
[◀](#)
[▶](#)
[Back](#)
[Close](#)
[Full Screen / Esc](#)
[Printer-friendly Version](#)
[Interactive Discussion](#)

Low pH and carbonate saturation state in the North Yellow Sea

W.-D. Zhai et al.

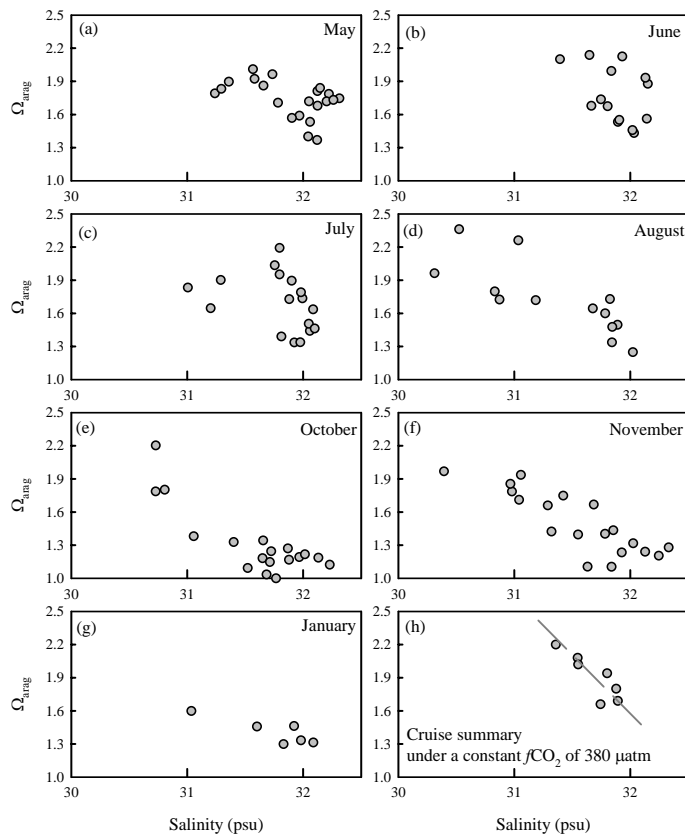


Fig. 15. Bottom water carbonate saturation state of aragonite (Ω_{arag}) versus salinity at deep stations (water depth > 25 m).

[Title Page](#)
[Abstract](#)
[Introduction](#)
[Conclusions](#)
[References](#)
[Tables](#)
[Figures](#)
[◀](#)
[▶](#)
[◀](#)
[▶](#)
[Back](#)
[Close](#)
[Full Screen / Esc](#)
[Printer-friendly Version](#)
[Interactive Discussion](#)

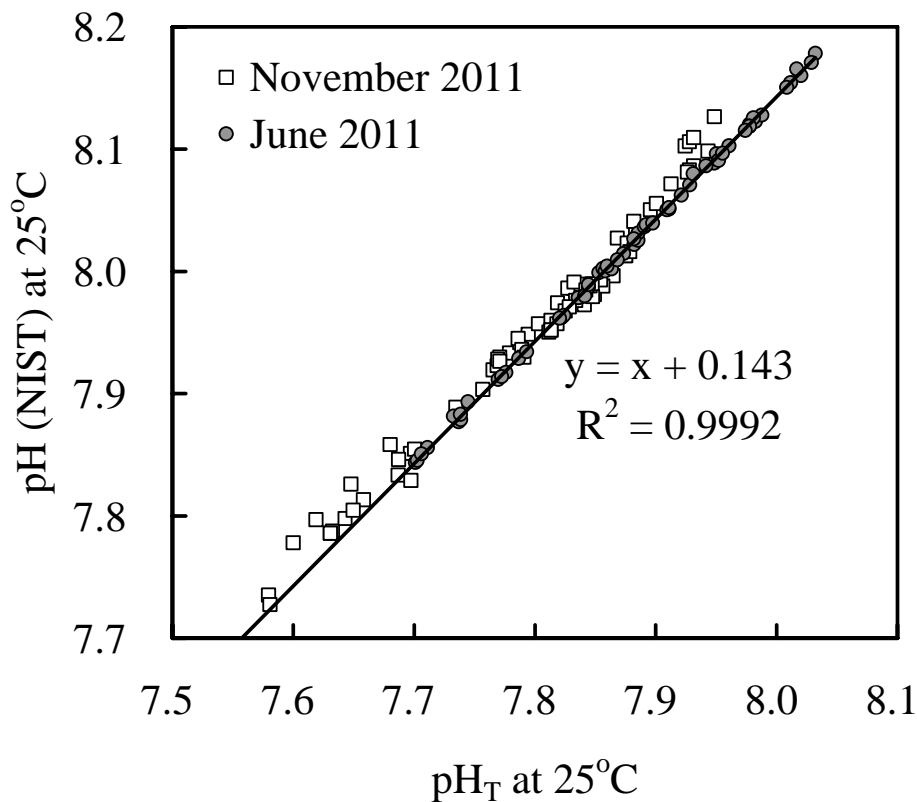


Fig. A1. Comparison between parallel pH measurements using total-hydrogen-ion scale pH buffers and NIST-traceable pH buffers.

Low pH and carbonate saturation state in the North Yellow Sea

W.-D. Zhai et al.

[Title Page](#)

[Abstract](#) [Introduction](#)

[Conclusions](#) [References](#)

[Tables](#) [Figures](#)

[⏪](#) [⏩](#)

[◀](#) [▶](#)

[Back](#) [Close](#)

[Full Screen / Esc](#)

[Printer-friendly Version](#)

[Interactive Discussion](#)



Low pH and carbonate saturation state in the North Yellow Sea

W.-D. Zhai et al.

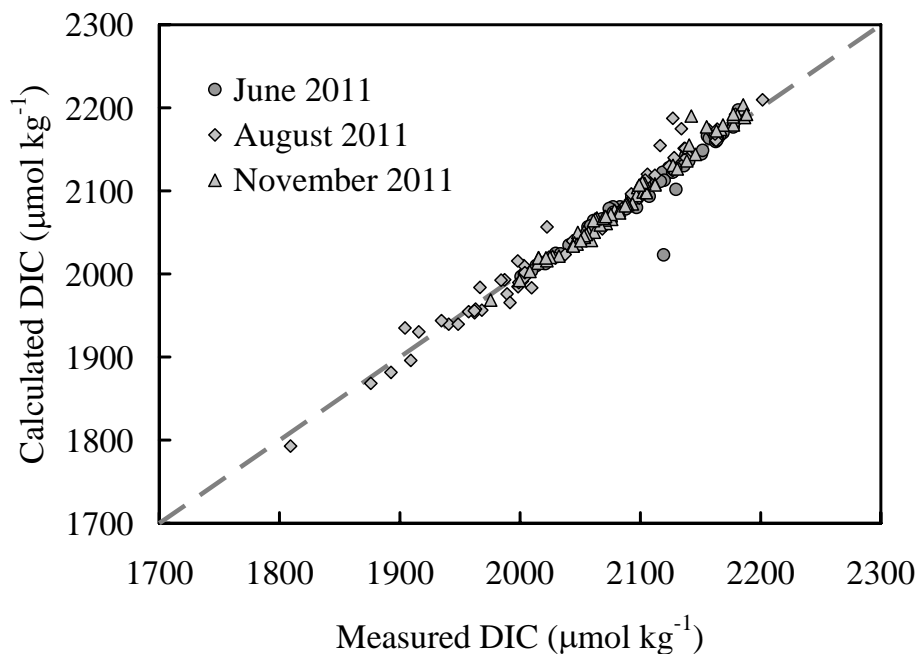


Fig. A2. Comparison between measured dissolved inorganic carbon (DIC) data and calculated DIC (from temperature, salinity, pH_T , and TAlk).

[Title Page](#)[Abstract](#)[Introduction](#)[Conclusions](#)[References](#)[Tables](#)[Figures](#)[⏪](#)[⏩](#)[◀](#)[▶](#)[Back](#)[Close](#)[Full Screen / Esc](#)[Printer-friendly Version](#)[Interactive Discussion](#)